JOURNAL OF GEOPHYSICAL RESEARCH, VOL. 106, NO. D23, PAGES 32,527–32,538, DECEMBER 16, 2001

Tropospheric ozone layers observed during PEM-Tropics B

Valérie Thouret[1], John Y. N. Cho, Mathew J. Evans[2], and Reginald E. Newell

Department of Earth, Atmospheric, and Planetary Sciences, Massachusetts Institute of Technology, Cambridge, Massachusetts

Melody A. Avery, John D. W. Barrick, Glen W. Sachse, and Gerald L. Gregory

NASA Langley Research Center, Hampton, Virginia

Abstract. In this paper we analyze distinct layers seen in the tropospheric ozone and water vapor profiles taken during NASA's Global Tropospheric Experiment (GTE) Pacific Exploratory Mission in the Tropical Pacific (PEM-Tropics) Phase B campaign. In summary, fewer layers were observed in this campaign than during the PEM-Tropics A campaign. However, of those layers found, there were relatively more ozone-rich-water-vapor-poor layers (68% versus 52%). The percentage of the sampled troposphere occupied by layers during PEM-Tropics B was less than half of that found during PEM-Tropics A (8% versus 20%). The differences between these two campaigns suggest a seasonal variation in the occurrence of layers. This is confirmed using measurements made by the Southern Hemisphere Additional Ozonesondes (SHADOZ) network.

1. Introduction

NASA's Global Tropospheric Experiment (GTE) Pacific Exploratory Mission in the Tropical Pacific (PEM-Tropics) Phase B took place during March and April 1999 and was designed to act as a sequel to PEM-Tropics A [*Hoell et al.*, 1999]. It involved two aircraft, the DC-8 and P-3B, operating from bases in Hawaii, Christmas Island, Tahiti, Fiji, and Easter Island. The objective was to investigate the chemistry of the remote tropical Pacific troposphere during the season opposite to the one sampled during PEM-Tropics A and over the same area. January–April is the wet season of the southern tropics, and biomass burning during that time of year is concentrated in the northern tropics [*Hao and Liu*, 1994]. This contrasts with September–October (the PEM-Tropics A period), which was during the dry season of the southern tropics, and the biomass burning season in the Southern Hemisphere. PEM-Tropics B was thus designed to provide an important complement to PEM-Tropics A. Ozonesonde data from Fiji, Tahiti, and Easter Island indicate lower O_3 levels in January–April than in September–October. This manifests itself in the large-scale minimum of tropospheric O_3 over the equatorial Pacific [*Routhier*, 1980; *Piotrowicz et al.*, 1991] being particularly extensive in January–April, stretching from the western Pacific warm pool to South America [*Fishman et al.*, 1990]. Although this region is remote, biomass burning may still influence the region due to long-range transport from the northern tropics.

To further the objectives of PEM-Tropics B [*Raper et al.*, this issue], this paper focuses on the tropospheric ozone and water vapor layers so as to allow comparison with the previously collected PEM data [*Newell et al.*, 1996; *Wu et al.*, 1997; *Stoller et al.*, 1999; *Newell et al.*, 1999]. In section 3 we will present a statistical analysis of this mission and then in subsequent sections discuss the differences with the PEM-Tropics A results following three complementary discussions.

In section 4, we compare the results with those made using the temporally more extensive Southern Hemisphere Additional Ozonesondes (SHADOZ) network of ozone and water vapor sondes [*Thompson and Witte*, 1999]. The advantage of these measurements is that they provide data collected over at least two years. Although in a geographically restricted region, they help place the PEM-Tropics A and B results into a better seasonal framework. As previously demonstrated by *Thouret et al.* [2000], there is a seasonal cycle in the occurrence of layers in this region, too. Are the differences

[1]Now at the Laboratoire d'Aérologie, Centre National de la Recherche Scientifique, Observatoire Midi-Pyrénées, Université Paul Sabatier, Toulouse, France.

[2]Now at the Department of Earth and Planetary Sciences, Harvard University, Cambridge, Massachusetts.

Paper number 2001JD900011.
0148-0227/01/2001JD900011$09.00

observed between the results of the two PEM-Tropics data set consistent with the seasonal cycle exhibited with the SHADOZ data?

In section 5 we use the SHADOZ data to investigate the robustness of our stastistical method. We aim to investigate how sensitive the statistics are to our definition of a layer.

In section 6 we discuss the differences in the meteorological conditions over the sampled area between PEM-Tropics A and B. In the previous studies we identified stratospheric intrusions and convection as the meteorological processes most likely to dominate the creation of ozone and water vapor layers in this region. This paper tries to use the differences between the observed layers during PEM-Tropics A and B, and the differences in the meteorology of these two campaigns to gain an understanding of what determines the creation and the number of these layers.

Although useful in itself, the existence of tropospheric trace constituent layers may be of importance for other activities. An important aspect of any field campaign is to create a data set against which chemical transport models (CTMs) can be compared. One of the major problems faced by such models concerns the horizontal and vertical resolution needed to adequately represent the important chemical and dynamical processes occurring in the troposphere. As the chemistry of ozone production and destruction is nonlinear with respect to NO_x, the large-scale mixing inherent in CTMs creates an obvious uncertainty. Understanding the small-scale structure of the atmosphere as it manifests itself in these layers is important if we are to have faith in the results calculated using such CTMs.

Recent studies have compared ozone production efficiencies when air masses of different origin were separated and when they were merged. The work of *Liang and Jacobson* [2000] suggest that ozone production may be overpredicted by as much as 60% in a model with coarse resolution compared to a finer resolution model. This effect is especially important in regions with strong concentration gradients. A similar study [*Esler et al.*, 2001] investigated the effect of mixing of ozone and water vapor across the tropopause. This suggested that if this rate was too high (as is expected in three-dimensional CTMs due to their limited grid resolution) there would be a large increase in the OH concentration in the tropopause region with a subsequent increase in the oxidation capacity in that region. Understanding the structures seen in the troposphere will help us to understand the resolution problems faced by the current generation of CTMs.

2. Data Set and Definition of Layer

We used data from 18 DC-8 flights (flight 5 to flight 22) and 16 P-3B flights (flight 3 to flight 19, except flight 12 for which data were unavailable). The initial flights for both aircraft were tests conducted out of

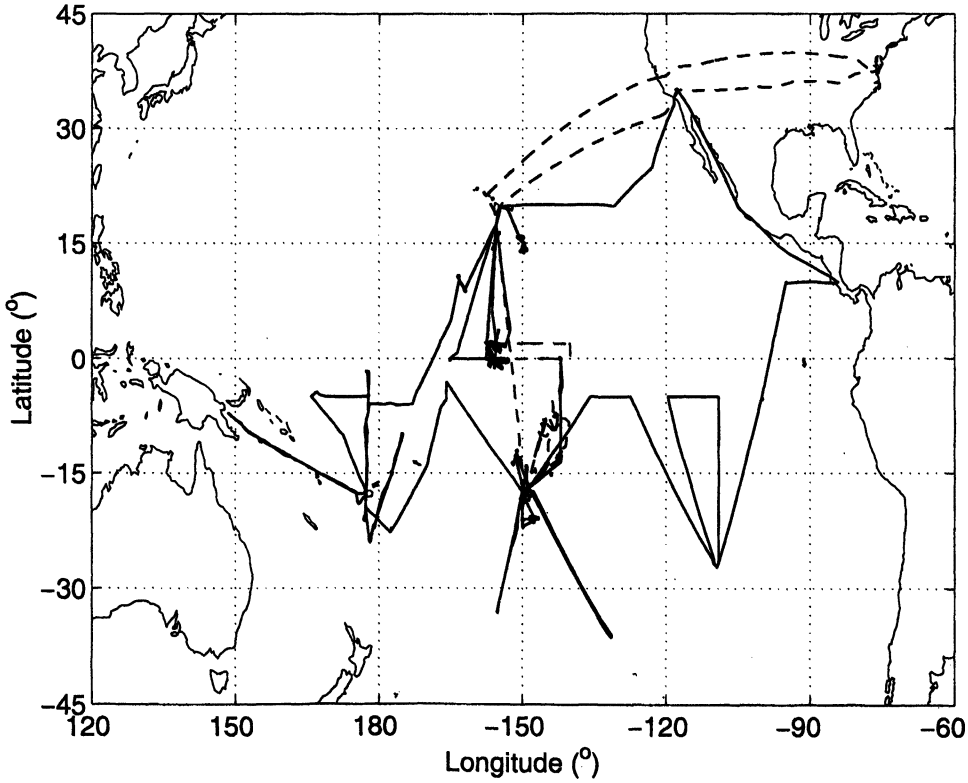

Figure 1. Map of the tracks of the DC-8 (solid) and P-3B (dashed) during PEM-Tropics B for flights that were used in this study.

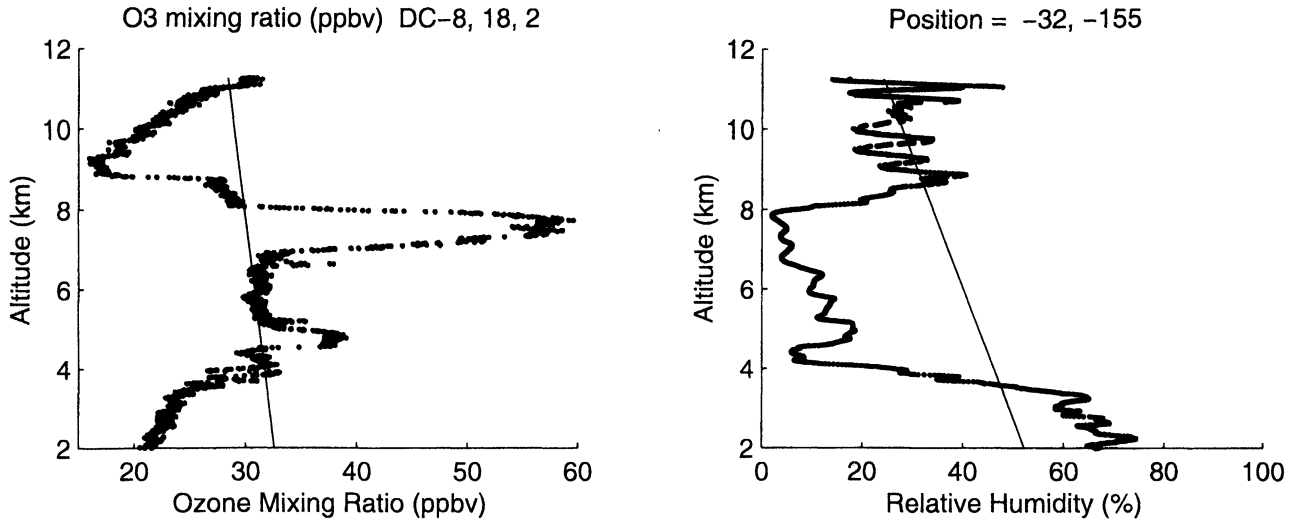

Figure 2. Example of ozone and water vapor vertical profiles recorded during flight 18 of the DC-8 operating on April 11, 1999, from Tahiti. Position given is latitude, longitude.

their respective home bases. Figure 1 shows the tracks of the DC-8 and the P-3B for the flights used in this study. The profiles were well distributed over the sampled area and reasonably characterize the tropical Pacific troposphere. 268 vertical profiles were performed in total for an average of ~8 profiles per flight, leading to over 1300 km of the troposphere being vertically sampled. Additional comments on the campaign and a description of the characteristics of the instrumentation are given by *Raper et al.* [this issue].

In order to analyze atmospheric layers a background concentration profile was defined for each profile made by the aircraft. Briefly, the linear trend was subtracted, the mode in the probability distribution function of the residuals found, then the linear trend restored to the mode bin to form the background profile (see *Stoller et al.* [1999] for a complete description). Layers in the ozone and water vapor profiles were identified from deviations exceeding specified thresholds from these background profiles. As opposed to the *Stoller et al.* [1999] paper, which used 5 ppbv for ozone, and to be consistent with the later papers dealing with tropospheric ozone layers [*Newell et al.*, 1999; *Thouret et al.*, 2000], we set the minimum deviations required for defining a layer in this study to be 10 ppbv for ozone and 5% relative humidity for water vapor. The altitude and thickness of the layers were calculated using the ozone profiles alone. The altitude of the layer is the altitude of the greatest ozone deviation, and the thickness is then determined by finding the two points where the ozone deviation falls to 5 ppbv on each side of the maximum deviation. If the ozone deviation does not fall to 5 ppbv on both sides, a layer is not recorded. The ozone layers are described as being greater or less than the background profile (we shall use the notation O_3+ or O_3- to identify these layers). Similarly, the water vapor may be greater or less than the background profile (again described as being H_2O+ or H_2O-). Using this approach, we can identify four different types of layers (O_3+ H_2O+, O_3+ H_2O-, O_3- H_2O+, and O_3- H_2O-). For both background calculations and layer analyses we neglected the lowest 2 km of the troposphere to avoid defining the boundary layer as a layer in our statistics. Note that hereafter, for the sake of brevity, "relative layer abundance" will mean "percentage of the vertically sampled space occupied by layers."

Figure 2 shows an example of ozone and water vapor vertical profiles plotted together with their associated backgrounds. In this particular example, there are three ozone deviations that could be construed as layers when examined by eye: one centered at ~9 km altitude, another at ~7.5 km, and a small one at ~5 km. The algorithm ignores the bottom one, because the deviation is < 10 ppbv. The middle one is defined as O_3+ H_2O-, which appears to be correct. The top one is classified as O_3- H_2O-, which is debatable given the ambiguous nature of the humidity deviations within that ozone layer. This example shows that there will clearly be some "noise" in the layer statistics. Sometimes what appears to the eye as a positive deviation may be classified as a negative deviation and vice versa. The number of layers detected will depend on the deviation threshold used (we will explore this sensitivity issue further in section 5). Obviously, there is no perfect method for defining layers, and, on the whole, the algorithm tends to agree with subjective visual inspections.

Plate 1 presents back trajectories associated with this flight (calculated using European Center for Medium-Range Weather Forecasts (ECMWF) meteorological fields and the code of *Methven* [1997]). It shows very well how the layers are created by the ability of the atmosphere to mix air masses with very different source regions. Three days earlier, the ozone-poor air mass at ~9 km altitude was in the marine boundary layer,

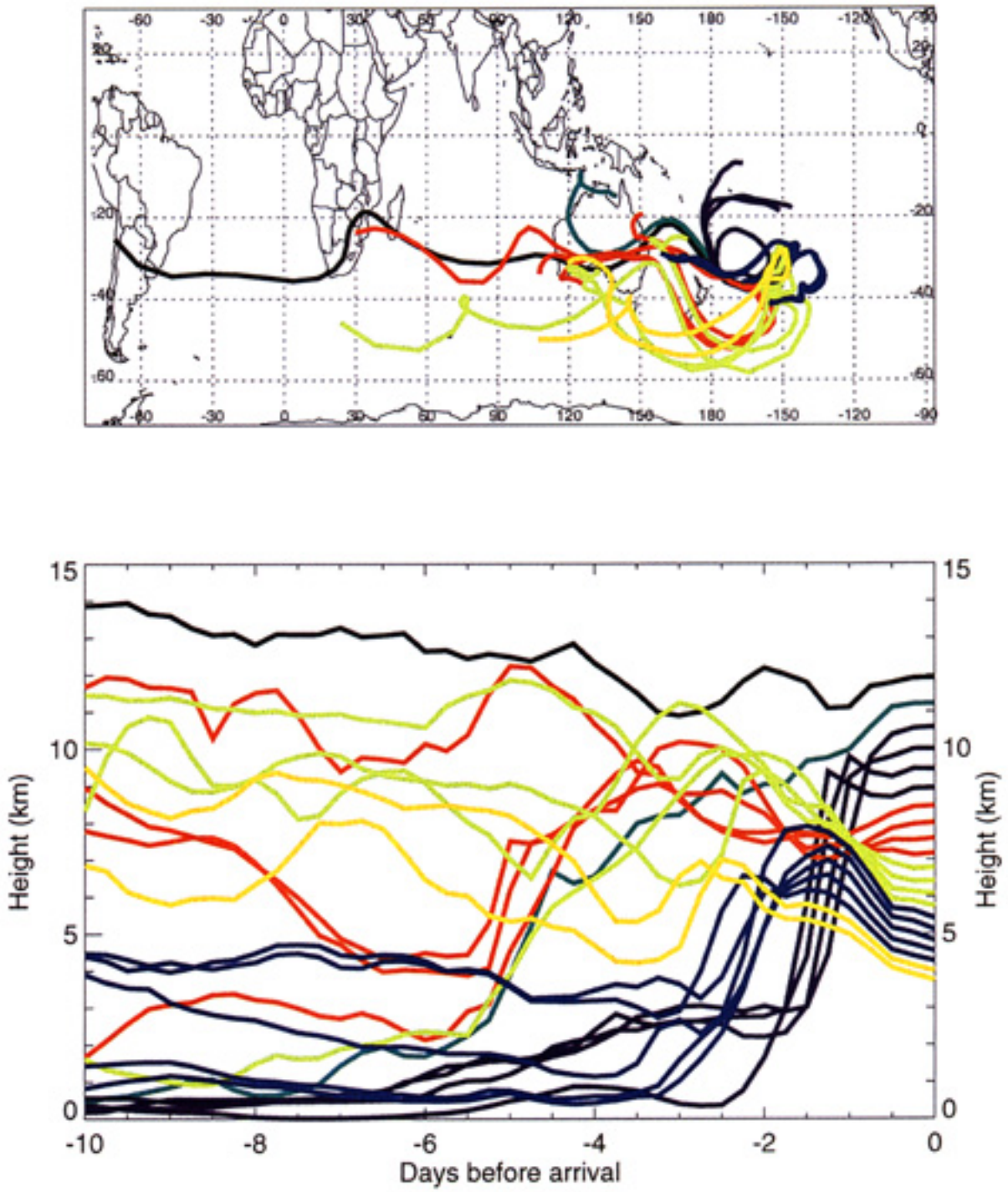

Plate 1. Ten-day back trajectories associated with flight 18 of the DC-8 operating on April 11, 1999, from Tahiti (calculated using ECMWF meteorological fields and the code of *Methven* [1997]).

Table 1. Layers Observed During PEM-Tropics B[a]

Layer Type	Observations	Percentage	Altitude, km	Thickness, km
Type 1: O_3+ H_2O+	14	7	6.6	0.40
Type 2: O_3+ H_2O−	133	68	5.6	0.49
Type 3: O_3− H_2O+	18	9	7.6	0.92
Type 4: O_3− H_2O−	31	16	7.2	0.57
Total/mean	196		6.1	0.54

[a]Total of ascent and descent checked for layers: 1330.06 km. Percentage of the troposphere occupied by layers: 8%. Altitude and thickness are means.

where it will have experienced rapid ozone loss and acquired high water vapor concentrations. The ozone-rich layer at ~8 km shows both a descent from the upper troposphere and an ascent from the lower troposphere 5–6 days earlier. Potential vorticity analysis made by *Browell et al.* [this issue] suggests that this air may well have had a stratospheric origin, but, on the other hand, the positive deviations of CO and CH_4 (not shown) suggest pollution. We can thus hypothesize that this layer was an example of the capping process (a pollution plume from the ground trapped by a stable layer of stratospheric origin) as proposed by *Stoller et al.* [1999]. Moreover, this example shows the way in which the atmosphere can bring air masses with very different chemical histories together. It is therefore not surprising that layers are observed extensively in the atmosphere.

3. Layers Observed During PEM-Tropics B: Statistical Results

3.1. Four Types of Layers: O_3 and H_2O

Table 1 shows a summary of the statistics calculated for the layers observed during the PEM-Tropics B flights. Table 1 can be compared to the ones presented by *Newell et al.* [1999], which give statistical results from the three previous PEM campaigns using the same layer definition. The first surprise concerns the percentage of the troposphere occupied by layers. From the previous campaigns, this number was between 14% (PEM-West A and B) and 20% (PEM-Tropics A). Here we calculate only 8%. The second surprise concerns the relative occurrence rates of the different layer types. During PEM-Topics A this was found to be 15, 50, 17, and 18% for the four types of layers O_3+ H_2O+, O_3+ H_2O−, O_3− H_2O+, and O_3− H_2O−. During PEM-Tropics B, even though we did not observe as large a fraction of the atmosphere taken up by layers, we saw a higher percentage of those layers to be ozone-rich-water-vapor-poor (type 2) than during previous campaigns.

3.2. Static Stability

Table 2 gives the statistical results when we include information about the static stability of the layer. This approach is described by *Thouret et al.* [2000] where the extensive Measurement of Ozone and Water Vapor by Airbus in-service aircraft (MOZAIC) database has been studied. (MOZAIC is an ongoing program that archives ozone and humidity data collected at 4-s intervals by five long-range commercial aircraft [*Marenco et al.*, 1998; *Thouret et al.*, 1998; *Cho et al.*, 1999a].) Briefly, as for ozone and water vapor, we defined automatically a background profile for each potential temperature profile. Then we compared the gradients for the bottom half (dry layers) or top half (wet layers) of the layer and outside the layer. In this way we obtain a new set of layer types, with each one of the previous ones divided into high or low stability within the layer, meaning that the static stability within the layer was higher or lower than the one corresponding to the background. The Table 2 results are similar to those calculated for the MOZAIC data. The more stable ozone-rich-water-vapor-poor (type 2+) layer is the most com-

Table 2. Layers Observed During PEM Tropics B: Including the Stability Criterion[a]

Layer Type	Observations	Percentage	Altitude, km	Thickness, km
Type 1+: O_3+ H_2O+ S+	6	3	5.5	0.26
Type 1−: O_3+ H_2O+ S−	8	4	7.5	0.52
Type 2+: O_3+ H_2O− S+	80	41	5.3	0.45
Type 2−: O_3+ H_2O− S−	53	27	6.1	0.57
Type 3+: O_3− H_2O+ S+	5	3	4.8	1.09
Type 3−: O_3− H_2O+ S−	13	7	8.7	0.85
Type 4+: O_3− H_2O− S+	10	5	6.4	0.20
Type 4−: O_3− H_2O− S−	21	11	7.5	0.74
Total/mean	196		6.1	0.54

[a]S+ is higher stability, S− is lower stability. Altitude and thickness are means.

Table 3. Layers (16 Types) Observed During PEM-Tropics B[a]

Layer Type	Observations	Percentage	Altitude, km	Thickness, km
Type 1A: O_3+ H_2O+ CO+ CH_4+	7	9	7.5	0.56
Type 1B: O_3+ H_2O+ CO+ CH_4−	1	1	6.7	0.61
Type 1C: O_3+ H_2O+ CO− CH_4+	1	1	4.5	0.32
Type 1D: O_3+ H_2O+ CO− CH_4−	0			
Type 2A: O_3+ H_2O− CO+ CH_4+	32	41	5.9	0.64
Type 2B: O_3+ H_2O− CO+ CH_4−	5	6	7.1	0.79
Type 2C: O_3+ H_2O− CO− CH_4+	7	9	7.5	0.67
Type 2D: O_3+ H_2O− CO− CH_4−	8	10	5.3	0.59
Type 3A: O_3− H_2O+ CO+ CH_4+	2	3	9.7	0.42
Type 3B: O_3− H_2O+ CO+ CH_4−	4	5	9.1	1.28
Type 3C: O_3− H_2O+ CO− CH_4+	3	4	4.8	1.28
Type 3D: O_3− H_2O+ CO− CH_4−	2	3	8.0	0.94
Type 4A: O_3− H_2O− CO+ CH_4+	1	1	8.3	0.23
Type 4B: O_3− H_2O− CO+ CH_4−	1	1	7.7	1.07
Type 4C: O_3− H_2O− CO− CH_4+	2	3	8.7	0.98
Type 4D: O_3− H_2O− CO− CH_4−	3	4	8.1	0.66
Total/mean	79		6.6	0.70

[a]Altitude and thickness are means.

mon type. Since high ozone/high stability/low water vapor is a signature of a layer extruding from the stratosphere into the troposphere (at least initially) [e.g., *Cho et al.*, 1999b], the results here reinforce the notion that stratospheric intrusions are one of the main physical processes creating layers.

3.3. Sixteen Types of Layers: O_3, H_2O, CO, and CH_4

To learn more about the origin of the air masses associated with these layers, we can use other trace gases measured aboard the aircraft. In this case we use the CO and CH_4 measured on the DC-8 (no measurements of CH_4 were made on the P-3B). The analysis methodology is the same for the CO and CH_4 as for the O_3 and H_2O. Background profiles are calculated and deviations above critical levels (3 ppbv for both CO and CH_4) are attributed to layers. By introducing the two extra variables (CO and CH_4) to the two already discussed (O_3 and H_2O) 16 different permutations of layer types are possible. Table 3 gives the decomposition of the 16 types of layers only using the DC-8 measurements. There are fewer layers in total than in Tables 1 and 2, not only because just the DC-8 data were used, but also because some of the previously defined layers did not have sufficient deviations in CO and CH_4 to be redefined as layers. As with the previous PEM data (see details by *Stoller et al.* [1999]), independent of the total number of layers, we can see that the most populous category of layers (with 41%) is of the O_3+H_2O− CO+CH_4+ type, which is indicative of pollution from the continental boundary layer. The dryness of the layer may be attributable to subsiding motion after the pollution was raised up by convection from the boundary layer. We also note that 10% of the layers show a "pure" stratospheric signature (O3+H2O−CO−CH_4−) compared to 3% during PEM-Tropics A, 3% during PEM-West A, and 21% during PEM-West B. (We recalculated the statistics presented by *Stoller et al.* [1999] using an ozone deviation threshold of 10 ppbv to be consistent with the current study and so that a comparison can be made.) The fact that the O_3+H_2O−CO+CH_4+ type is the most populous category does not necessarily contradict the fact that we also mostly observe O_3+H_2O−S+ layers. As stated previously, this may indicate that the capping process is common in the troposphere. Stable stratospheric air may trap polluted plumes coming from the boundary layer. The two air masses are then mixed together and we can observe both the stratospheric and the polluted boundary layer characteristics in the same (for our algorithm) layer. Indeed, a recent study from *Parrish et al.* [2000] has reported a case of close proximity of air masses with contrasting source signature: high levels of anthropogenic pollution immediately adjacent to elevated ozone of stratospheric origin.

4. Seasonal Cycles Using SHADOZ and MOZAIC Data

The large difference between the number of layers observed during PEM-Tropics A and B and the large differences in the meteorological situation between these two campaigns suggest that the number of layers seen in this region may show a seasonal variation. A recent study from *Thouret et al.* [2000] has shown the existence of large and robust seasonal cycles in layer diagnostics in other regions of the world. The measurements made during PEM-Tropics A and B cannot in themselves establish the existence of a robust seasonal cycle as they cover only a few months of the year. Alternative data sets are required to establish the seasonal cycle of these diagnostics.

The SHADOZ network of ozonesondes provides such a data set (for details see the Web site: http://code 916.gsfc.nasa.gov/Data_services/shadoz/Shadoz_hmpg2

.html). These ozonesondes are released from various locations in the southern hemisphere tropics and offer coverage from at least 1998 to 1999. The data in the tropical Pacific (Tahiti, Fiji, Samoa) are especially valuable for comparing with the PEM-Tropics data set. The same definition of layers and the same statistics algorithm have been applied to these data from the three SHADOZ sites in order to assess the seasonal cycle of these statistics in this region. A total of 253 soundings (almost equally divided between the three sites) have been analyzed to obtain this statistic. Figure 3 shows the seasonal cycle of the percentage of the vertically sampled space occupied by layers. We note that the relative layer abundance is much less in March–April (the PEM-Tropics B period) than in September–October (the PEM-Tropics A period). The relative layer abundance obtained from the SHADOZ network data is very similar to the ones calculated with the PEM data for the two periods of sampling as shown in Figure 3.

Strong seasonal cycles were manifest in the MOZAIC data from all subregions as well [*Thouret et al.*, 2000]. It is therefore curious that such a difference was not observed between the PEM-West A and B campaigns. These missions were also carried out during opposite seasons but in the western Pacific, mostly at midlatitudes [*Hoell et al.*, 1996, 1997]. The observed seasonal cycle from MOZAIC may explain why. Figure 4 shows the seasonal cycle of the relative layer abundance calculated with the MOZAIC data set selecting only those measurements at midlatitudes. This cycle shows a maximum (~25%) in summer and a minimum (~8%) in winter. The PEM-West missions were conducted in March-April and September-October, and as we see from the MOZAIC measurements, these two opposite seasons show the same abundance of layers, which is close to 14% as it has been calculated with the PEM-West data set. Thus the lack of a seasonal cycle in the PEM-West data is consistent with the seasonal cycle calculated in other campaigns.

5. Sensitivity of Statistics to Ozone Threshold

The minimum mean ozone concentrations occur between February and April in the PEM-Tropics region. This has been observed in both satellite measurements [*Fishman et al.*, 1990] and from the SHADOZ network data. Figure 5 shows the ozone concentration at an altitude of 5 km calculated from all the soundings launched at Tahiti, Fiji, and Samoa as part of the SHADOZ program. This ozone cycle shows a maximum in September–October related to the period of intense biomass burning in the southern tropics and shows a minimum in January–April. This ozone seasonal cycle at 5 km altitude is in agreement with the mean ozone concentrations that we calculated for the two PEM-

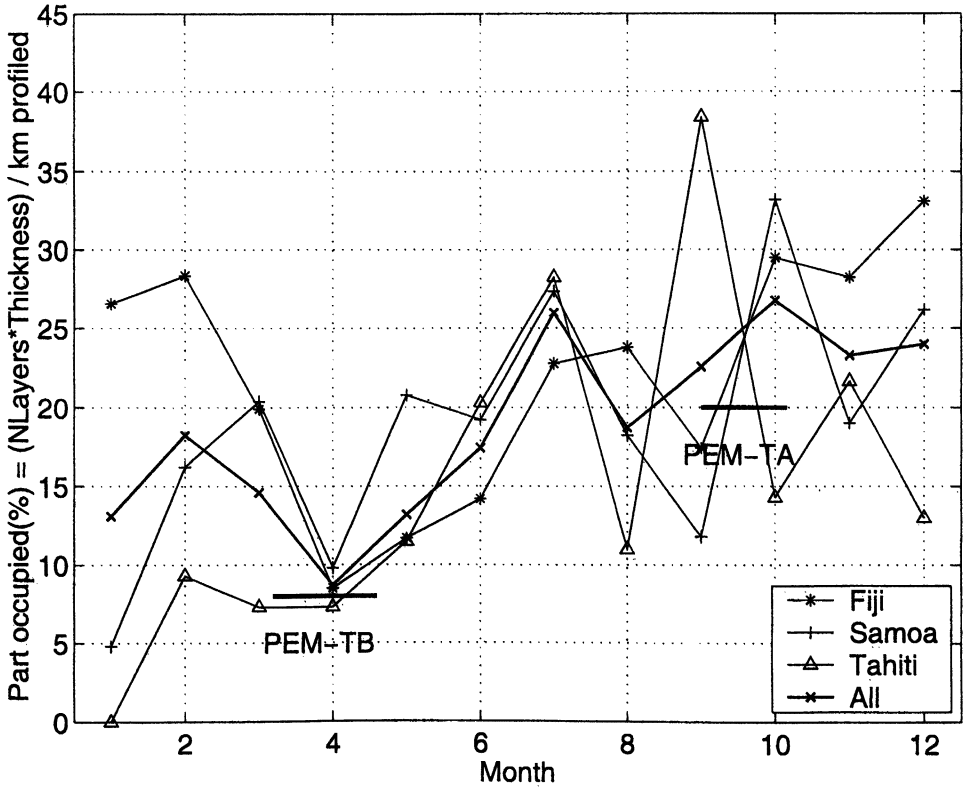

Figure 3. Seasonal cycle of the percentage of the vertically sampled space occupied by layers ("relative layer abundance") based on 2 years of measurements (1998–1999) from the three SHADOZ sites: Fiji, Samoa, and Tahiti.

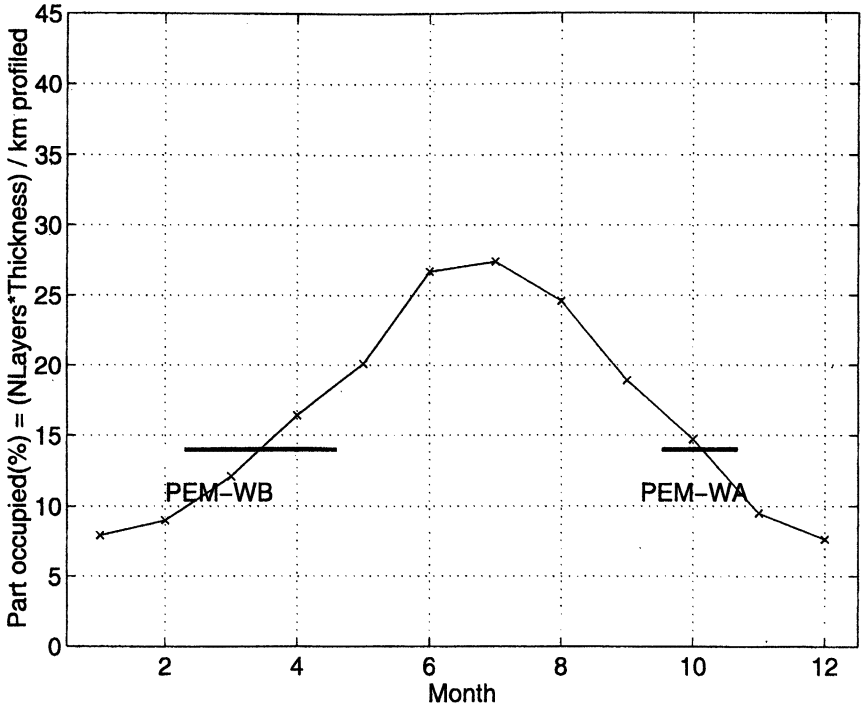

Figure 4. Seasonal cycle of the relative layer abundance based on the MOZAIC measurements for the years 1994 to 1997.

Tropics data sets (~40 ppbv during PEM-Tropics A and 25 ppbv during PEM-Tropics B). It is interesting to note that this seasonal cycle in mean ozone has a similar shape to the seasonal cycle in the relative layer abundance (see Figure 3). To ensure the robustness of the seasonal cycle found in the number of layers in the troposphere, we analyze the influence of the minimum ozone deviation (MinO3dev) required to define

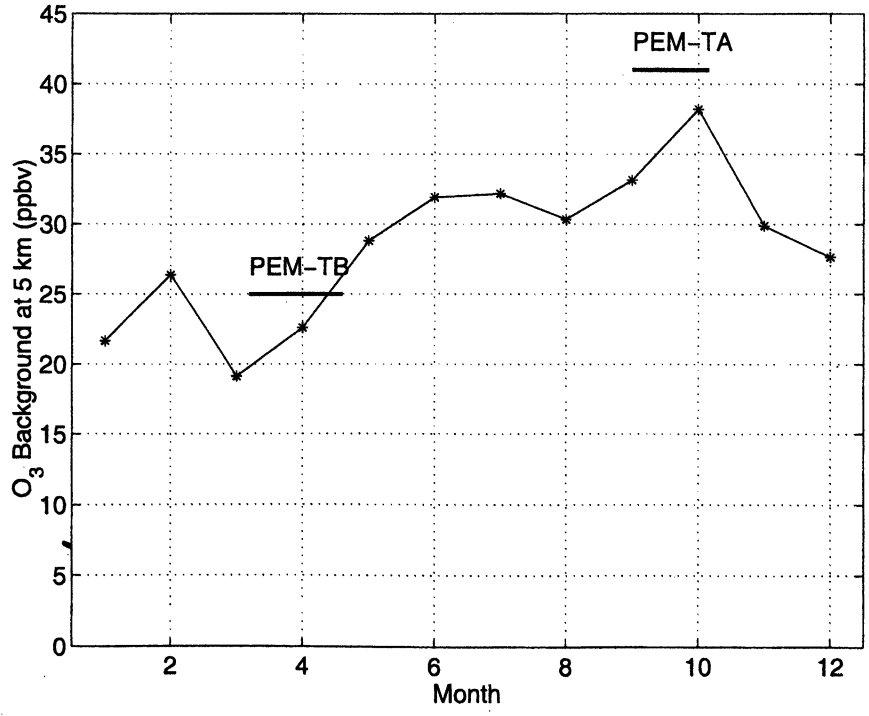

Figure 5. Mean ozone concentration at 5-km altitude calculated from all the soundings launched at Tahiti, Fiji, and Samoa in 1998 and 1999 as part of the SHADOZ program. Mean values (using all altitudes) are shown for the PEM-Tropics A and B data sets as reference.

Table 4. Layers Observed During PEM-Tropics B[a]

Layer Type	Observations	Percentage	Altitude, km	Thickness, km
Type 1: O_3+ H_2O+	84	15	6.4	0.35
Type 2: O_3+ H_2O−	320	55	5.4	0.49
Type 3: O_3− H_2O+	95	16	6.1	0.57
Type 4: O_3− H_2O−	84	14	6.2	0.41
Total/mean	583		5.7	0.47

[a]Ozone minimum deviation is 5 ppbv. Total of ascent and descent checked for layers: 1330.06 km. Part of the troposphere occupied by layers: 20%. Altitude and thickness are means.

a layer in our algorithm. (What we call relative layer abundance is similar to the number of layers because the layer thickness has no seasonal cycle as shown by *Thouret et al.* [2000].) As described previously, we fixed this deviation at 10 ppbv for ozone. If we lower this threshold to 5 ppbv for ozone and still use 5% relativity humidity for water vapor, the layer statistics for PEM-Tropics B becomes similar to those for PEM-Tropics A when using 10 ppbv for ozone. Table 4 gives these new statistics for PEM-Tropics B. They are surprisingly similar.

Since MinO3dev clearly affects the number of layers detected, we decided to use an ozone deviation threshold that is a quarter of the ozone mean concentration at 5 km altitude taken from the SHADOZ network measurements (Figure 5) in order to be consistent with the fact that we took 10 ppbv for PEM-Tropics A, while the ozone concentration was maximum (~40 ppbv), and 5 ppbv for PEM-Tropics B when ozone was minimum (~20 ppbv). Figure 6 presents the seasonal cycles of the number of layers both when the algorithm used a MinO3dev of 10 ppbv for each month, when the algorithm used a MinO3dev that was a quarter of the mean ozone for each month, and when the algorithm used a MinO3dev of 5 ppbv for each month.

The three lines are not dramatically different in shape, which is reassuring. This suggests that our statistics are reasonably robust. There is little influence on our choice of MinO3dev on the conclusions that we have made. We may be able to gain more insight

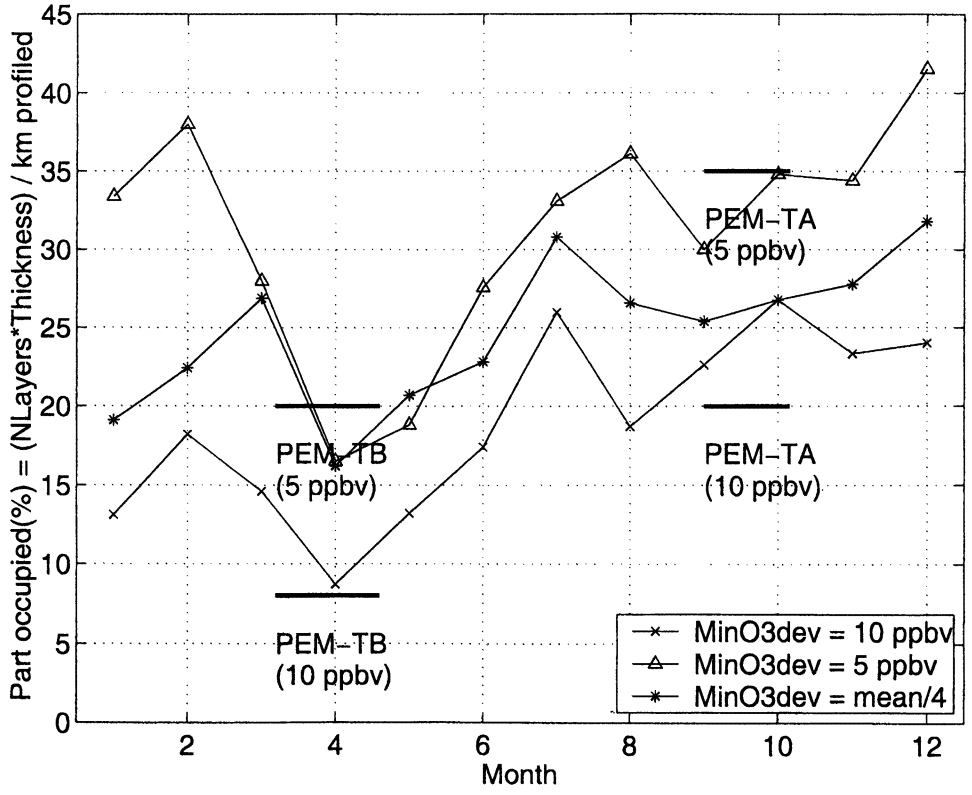

Figure 6. Seasonal cycles of the relative layer abundance when the algorithm uses a MinO3dev of 10 ppbv for each month, 5 ppbv for each month, and a quarter of the mean ozone for each month.

from this result. By having a MinO3dev that varies with the mean O_3 we may have factored out the seasonal variation in ozone production to some extent. If this were the case and there was no seasonal variation in the meteorological parameters associated with layer production, we might expect the seasonal cycle of the relative layer abundance to be flat. However, we still see a seasonal cycle in both the case with the constant MinO3dev and a varying MinO3dev, which suggests that possibly it is the meteorological or geographical aspects of the layer production/destruction that is more important than any chemical effects. This is somewhat speculative, however.

6. Interpretation of the Differences Between PEM-Tropics A and PEM-Tropics B

In this section we will briefly examine both the major chemical and meteorological differences between the two missions, and the impact these differences may have on trace constituent layers in the troposphere. The PEM-Tropics A campaign emphasized the importance of biomass burning in the southern hemisphere and the location of the intertropical convergence zone (ITCZ) and the South Pacific convergence zone (SPCZ) in determining the composition of the atmosphere. We will discuss how changes in these parameters are reflected in the statistics we described earlier in this paper.

6.1. Chemistry

During PEM-Tropics A, biomass burning in the southern hemisphere tropics (South America, southern Africa, and northern Australia) played a significant role in determining the composition of the atmosphere over the tropical Pacific [*Hoell et al.*, 1999; *Schultz et al.*, 1999]. This is the dry season for these locations and satellite-based fire counts show that this is the maximum period of biomass burning in the southern hemisphere tropics. This contrasts with the PEM-Tropics B period, which is the wet season for the southern hemisphere tropics and biomass burning is at a minimum. In the Northern Hemisphere tropics the situation is reversed. PEM-Tropics B occurred during the dry season (spring) in the Northern Hemisphere and so during the maximum of the northen hemisphere biomass burning (predominantly in northern Africa below the Sahara and southeast Asia). PEM-Tropics A occurred during the northern tropical wet season and so little or no biomass burning took place there. So it might be reasonable to expect a change in layer statistics based on the change in ozone sources alone. That is, one might expect a reduction in O_3+ layers with a decrease in ozone sources.

6.2. Meteorology

Fuelberg et al. [this issue] give a meteorological overview of PEM-Tropics B, and the authors also assess the differences between the two missions. One of the major differences is the activity of the ITCZ and the SPCZ. During PEM-Tropics A, both of these features were more clearly defined from the divergent wind component at low levels than were observed during PEM-Tropics B. However, the ITCZ had a double-walled structure during PEM-Tropics B (convection strips just north and south of an equatorial subsidence zone) [*Hu et al.*, this issue], and may have provided an extra barrier to interhemispheric transport. This would have decreased the mixing of pollutants from the Northern Hemisphere (where, in this season, the biomass burning is occurring) to the Southern Hemisphere, where the creation of polluted layers would be reduced.

Convection probably plays a dual role in layer formation/destruction. On one hand, convection at a surface source of ozone (or a surface sink like the tropical marine boundary layer) would help form layers by pumping either ozone-rich or ozone-poor air to higher levels until flattened by stratification or stretched by vertical shear. On the other hand, convection through an already existing layer can destroy it by vertical mixing. The latter mechanism may have contributed to the relative dearth of layers during PEM-Tropics B, since greater vertical moisture fluxes in the sampled region (compared to during PEM-Tropics A) [*Hu et al.*, this issue] suggest more vertical mixing locally where the layers were sampled. Therefore, again from the meteorology alone we might expect a minimum in the occurrence of layers in the tropical Pacific during this period.

6.3. Future

A wholly convincing explanation of the mechanisms leading to the production, maintenance, and destruction of atmospheric layers is not possible at the moment. We cannot in any quantitative way describe the relative importance of any process in producing or destroying layers. It is thought that these mechanisms rely upon both meteorological and chemical processes that act on a large variety of both timescales and length scales. It is hoped that by using CTMs at sufficiently high resolution, the relative roles of meteorology (convection and frontal systems) and chemistry (ozone production and destruction) in producing layers may be elucidated quantitatively.

7. Summary Discussion

The PEM-Tropics B mission conducted in March–April 1999 concluded the PEM series by surveying the atmosphere over the South Pacific during the southern tropical wet season. This corresponded with the minimum in the seasonal cycle of ozone in the western equatorial Pacific reflecting the minimum in biomass burning.

Tropospheric ozone layers have been studied with the four PEM data sets. The results from PEM-Tropics A and B exhibit the strong seasonal cycle in the abundance of layers in the troposphere seen recently with the

extensive MOZAIC data set [*Thouret et al.*, 2000], with PEM-Tropics A showing a maximum and PEM-Tropics B displaying a minimum. This apparent seasonal variation is supported by 2 years of SHADOZ ozonesonde data from the same region. The sounding data exhibit the same features as the PEM-Tropics data in the statistics on layers and mean ozone concentrations. With this dataset we were also able to study the influence of the ozone deviation threshold used in the layer detection algorithm. Although this minimum threshold influences the number of layers seen it does not strongly alter the shape of the seasonal cycle of the relative layer abundance. This suggests that the occurrence of these layers is not only linked to the ozone sources and sinks but also to the meteorological conditions.

Interpreting the differences in the layer statistics between PEM-Tropics A and B is difficult. We would expect to see fewer pollution layers due to the reduction in the influence of biomass burning on the area, which may have been aided by the suppression of interhemispheric transport by the double-walled ITCZ. The reduction in relative layer abundance during PEM-Tropics B may also have been caused by an increase in vertical mixing in the sampling region (which could have increased the layer dissipation rate) as evidenced by a greater vertical moisture flux in the south tropical Pacific.

We have collected extensive statistics on a variety of observationally based parameters for layers in the troposphere and have speculated on the mechanisms leading to the production, maintenance, and destruction of these layers. It would seem like a good moment to attempt a more complex synthesis of this data. CTMs offer the next approach to understanding these layers. Attempting to reproduce these layers will provide a unique challenge to both the dynamics and chemistry of these models.

Acknowledgments. The MIT work was funded by NASA grant NAG1-2173 and NSF grant ATM 9910244. We would like to thank Yuanlong Hu for helpful discussions.

References

Browell, E. V., et al., Large-scale air mass characteristics observed over the remote tropical Pacific ocean during March-April 1999: Results from PEM-Tropics B field experiment, *J. Geophys. Res.*, this issue.

Cho, J. Y. N., R. E. Newell, V. Thouret, A. Marenco, and H. G. Smit, Trace gas study accumulates 40 million frequent-flyer miles for science, *Eos Trans. AGU*, *80*, 377–384, 1999a.

Cho, J. Y. N., et al., Observations of convective and dynamical instabilities in tropopause folds and their contribution to stratosphere-troposphere exchange, *J. Geophys. Res.*, *104*, 21,549–21,568, 1999b.

Esler, J. G., D. G. H. Tan, P. H. Haynes, M. J. Evans, K. S. Law, and J. A. Pyle, Stratosphere-troposphere exchange: Chemical sensitivity to mixing, *J. Geophys. Res.*, *106*, 4717–4731, 2001.

Fishman, J., C. E. Watson, J. C. Larsen, and J. A. Logan, Distribution of tropospheric ozone determined from satellite data, *J. Geophys. Res.*, *95*, 3599–3617, 1990.

Fuelberg, H. E., R. E. Newell, D. J. Westberg, J. C. Maloney, J. R. Hannan, B. C. Martin, and Y. Zhu, A meteorological overview of the second Pacific Exploratory Mission (PEM) in the Tropics, *J. Geophys. Res.*, this issue.

Hao, W. M., and M.-H. Liu, Spatial and temporal distribution of tropical biomass burning, *Glob. Biogeochem. Cycles*, *8*, 495–503, 1994.

Hoell, J. M., D. D. Davis, S. C. Liu, R. E. Newell, M. Shipham, H. Akimoto, R. J. McNeal, R. J. Bendura, and J. W. Drewry, Pacific Exploratory Mission West-A (PEM West-A): September-October 1991, *J. Geophys. Res.*, *101*, 1641–1653, 1996.

Hoell, J. M., D. D. Davis, S. C. Liu, R. E. Newell, H. Akimoto, R. J. McNeal, and R. J. Bendura, The Pacific Exploratory Mission-West, Phase B: February-March 1994, *J. Geophys. Res.*, *102*, 28,223–28,239, 1997.

Hoell, J. M., D. D. Davis, D. J. Jacob, M. O. Rodgers, R. E. Newell, H. E. Fuelberg, R. J. McNeal, J. L. Raper, and R. J. Bendura, Pacific Exploratory Mission in the tropical Pacific: PEM-Tropics A, August-September 1996, *J. Geophys. Res.*, *104*, 5567–5583, 1999.

Hu, Y., R. E. Newell, and Y. Zhu, Mean moist circulation for PEM-Tropics missions, *J. Geophys. Res.*, this issue.

Liang, J., and M. Z. Jacobson, Effects of subgrid segregation on ozone production efficiency in a chemical model, *Atmos. Environ.*, *34*, 2975–2982, 2000.

Marenco, A., et al., Measurement of ozone and water vapor by Airbus in-service aircraft: The MOZAIC airborne program, An overview, *J. Geophys. Res.*, *103*, 25,631–25,642, 1998.

Methven, J., Offline trajectories: Calculations and Accuracy, *Universities Global Atmospheric Modelling Programme Technical report No. 44.*, 1997, available from Centre for Global Atmospheric Modelling, University of Reading, Earley Gate, Reading RG6 6BB, UK.

Newell, R. E., et al., Vertical fine-scale atmospheric structure measured from NASA DC-8 during PEM-West A, *J. Geophys. Res.*, *101*, 1943–1960, 1996.

Newell, R. E., V. Thouret, J. Y. N. Cho, P. Stoller, A. Marenco, and H. G. Smit, Ubiquity of quasi-horizontal layers in the troposphere, *Nature*, *398*, 316–319, 1999.

Parrish, D. D., et al., Mixing of anthropogenic pollution with stratospheric ozone: A case study from the North Atlantic wintertime troposphere, *J. Geophys. Res.*, *105*, 24,363–24,374, 2000.

Piotrowicz, S. R., H. F. Bezdek, G. R. Harvey, Y. M. Springer, and K. J. Hanson, On the ozone minimum over the equatorial Pacific Ocean, *J. Geophys. Res.*, *96*, 18,679–18,687, 1991.

Raper, J. L., M. Kleb, D. Jacob, D. D. Davis, R. E. Newell, H. E. Fuelberg, R. J. Bendura, J. M. Hoell, and R. J. McNeal, Pacific Exploratory Mission in the tropical Pacific: PEM-Tropics B, March–April 1999, *J. Geophys. Res.*, this issue.

Routhier, F., Free tropospheric and boundary layer airborne measurements of ozone over the latitude range of 58°S-70°N, *J. Geophys. Res.*, *85*, 7307–7321, 1980.

Schultz, M. G., et al., On the origin of tropospheric ozone and NO_x over the tropical South Pacific, *J. Geophys. Res.*, *104*, 5829–5843, 1999.

Stoller, P., et al., Measurements of atmospheric layers from the NASA DC-8 and P-3B aircraft during PEM-Tropics A, *J. Geophys. Res.*, *104*, 5745–5764, 1999.

Thompson, A. M., and J. C. Witte, SHADOZ (Southern Hemisphere ADditional OZonesondes): A new data set for the Earth Science Community, *Earth Observer*, *11*, 27–30, 1999.

Thouret, V., A. Marenco, P. Nédélec, and C. Grouhel, Ozone climatologies at 9–12 km altitude as seen by the

MOZAIC airborne program between September 1994 and August 1996, *J. Geophys. Res.*, *103*, 25,653–25,679, 1998.

Thouret, V., J. Y. N. Cho, R. E. Newell, A. Marenco, and H. G. J. Smit, General characteristics of tropospheric trace constituent layers observed in the MOZAIC program, *J. Geophys. Res.*, *105*, 17,379–17,392, 2000.

Wu, Z.-X., R. E. Newell, Y. Zhu, B. E. Anderson, E. V. Browell, G. L. Gregory, G. W. Sachse, and J. E. Collins Jr., Atmospheric layers measured from the NASA DC-8 during PEM-West B and comparison with PEM-West A, *J. Geophys. Res.*, *102*, 28,353–28,365, 1997.

M. A. Avery, J. D. W. Barrick, G. L. Gregory, and G. W. Sachse, NASA Langley Research Center, Mail Stop 483, Hampton, VA 28681-2199. (m.a.avery@larc.nasa.gov; j.d.barrick@larc.nasa.gov; gregory@widomaker.com; g.w.sachse@larc.nasa.gov)

J. Y. N. Cho and R. E. Newell, Department of Earth, Atmospheric, and Planetary Sciences, Massachusetts Institute of Technology, 77 Massachusetts Ave., Rm. 54-1823, Cambridge, MA 02139-4307. (jcho@pemtropics.mit.edu; renewell@mit.edu)

M. J. Evans, Department of Earth and Planetary Sciences, Harvard University, 109A Pierce Hall, Oxford St., Cambridge, MA 02138. (mje@io.harvard.edu)

V. Thouret, Laboratoire d'Aérologie, CNRS (UMR 5560), OMP, UPS, 14 Avenue Edouard Belin, 31400 Toulouse, France. (thov@aero.obs-mip.fr)

(Received September 8, 2000; revised January 8, 2001; accepted January 9, 2001.)